Published in final edited form as:
J Neurosci. 2012 June 6; 32(23): 7862–7868. doi:10.1523/JNEUROSCI.0167-12.2012.

Emergence of coordinated plasticity in the cochlear nucleus and cerebellum

Hua Yang and **Matthew A. Xu-Friedman***
Dept. Biological Sciences, University at Buffalo, SUNY, Buffalo, NY 14260

Abstract

Synapses formed by one cell type onto another cell type tend to show characteristic short-term plasticity, which varies from facilitating to depressing depending on the particular system. Within a population of synapses, plasticity can also be variable, and it is unknown how this plasticity is determined on a cell-by-cell level. We have investigated this in the mouse cochlear nucleus, where auditory nerve (AN) fibers contact bushy cells (BCs) at synapses called “endbulbs of Held”. Synapses formed by different AN fibers onto one BC had plasticity that was more similar than would be expected at random. Experiments using MK-801 indicated that this resulted in part from similarity in the presynaptic probability of release. This similarity was not present in immature synapses, but emerged after the onset of hearing. In addition, this phenomenon also occurred at excitatory synapses in the cerebellum. This indicates that postsynaptic cells coordinate the plasticity of their inputs, which suggests that plasticity is of fundamental importance to synaptic function.

Introduction

Different synapses in the nervous system commonly exhibit different forms of short-term synaptic plasticity. This is even observed when one neuron makes synapses onto multiple target cell types, a phenomenon referred to as target-cell-specific synaptic plasticity (Markram et al., 1998; Reyes et al., 1998; Rozov et al., 2001). Synaptic plasticity may provide different computational characteristics to synapses. For example, depression has been proposed to make postsynaptic cells sensitive to changes in presynaptic activity levels, whereas facilitation makes postsynaptic cells more responsive to bursts of presynaptic activity (Fortune and Rose, 2002; Abbott and Regehr, 2004). In addition, depression may prevent highly active inputs from dominating postsynaptic activity (Abbott et al., 1997). Thus, the short-term plasticity at a synapse could reflect the specific computational interactions between particular cell types.

Plasticity is somewhat variable from one synapse to another within a population, which could provide finer tuning of these computational characteristics. This fine-tuning would be influenced by how much plasticity varies for the multiple synapses that converge onto the same postsynaptic cell. If plasticity is uniform, then activity from synaptic inputs will be filtered similarly, whereas if it is not, then some inputs could come to dominate the cell’s output.

These functional implications presume that plasticity is regulated, such as during development. Some synapses, such as the retinogeniculate synapse (Chen and Regehr, 2000) or cerebellar mossy fiber (Wall, 2005), show small shifts in plasticity over development, whereas the calyx of Held synapse in the medial nucleus of the trapezoid body (MNTB)

*Corresponding author: Phone: 716-645-4992, Fax: 716-645-2975, mx@buffalo.edu.

shows large changes (Taschenberger and von Gersdorff, 2000; Joshi and Wang, 2002; Taschenberger et al., 2002). However, it is not clear whether these findings indicate that plasticity is specifically regulated.

We have addressed these issues by studying excitatory synapses formed by auditory nerve (AN) fibers onto bushy cells (BCs) in the anteroventral cochlear nucleus (AVCN) (called the "endbulb of Held") (Lorente de Nó, 1981; Ryugo and Fekete, 1982; Limb and Ryugo, 2000). At the endbulb, the extent of depression varies considerably, which can have consequences for the transmission of information across the synapse (Yang and Xu-Friedman, 2009). In an initial study, we found that there was similarity in plasticity between converging endbulbs (Yang and Xu-Friedman, 2009). Here we address whether this similarity occurs pre- or post-synaptically, and how it emerges during development. In addition, we surveyed excitatory synapses in the cerebellum and found similarity among converging synapses, suggesting this phenomenon may be widespread in the nervous system.

Materials and Methods

Brain slices of the cochlear nucleus or cerebellum of CBA/CaJ mice of either sex were prepared as described previously (Xu-Friedman and Regehr, 2005; Yang and Xu-Friedman, 2008). BCs and cerebellar granule cells (GCs) were recorded in parasagittal slices, while Purkinje cells (PCs) and cerebellar stellate cells (SCs) were recorded in transverse slices. Recordings were made at 34°C in ACSF containing (in mM): 125 NaCl, 26 $NaHCO_3$, 1.25 NaH_2PO_4, 2.5 KCl, 20 glucose, 1 $MgCl_2$, 1.5 $CaCl_2$, 4 Na L-lactate, 2 Na-pyruvate and 0.4 Na L-ascorbate bubbled with 95% O_2 : 5% CO_2 (pH 7.4, 310 mOsm). The voltage-clamp solution contained (in mM): 35 CsF, 100 CsCl, 10 EGTA, 10 HEPES, and 1 QX-314. Pipettes were 1–2 MΩ for BCs and PCs, and 2–3 MΩ for SCs and GCs with series resistances of 12 MΩ, compensated to 70%. Cells were held at −70 mV (for AMPA EPSCs) or +40 mV (for NMDA EPSCs). BCs were distinguished from T-stellate cells in the AVCN by their EPSC decay kinetics and paired-pulse depression (Chanda and Xu-Friedman, 2010). Two separate stimulation isolation units (A365, World Precision Instruments) were used to stimulate separate synaptic inputs/pathways. Small glass pipettes were used, which contained normal ACSF. Stimulation and recording were controlled by mafPC, run in Wavemetrics Igor. Reliable fiber isolation was confirmed by the absence of sharp drops or increases in EPSC amplitude, particularly during trains. Trials on which a stimulus failed to trigger an EPSC were discarded. If there were sudden increases in amplitude, this presumably reflected stimulation of multiple inputs, and the stimulus electrode was moved. Independence of inputs was verified using cross-stimulation experiments, that is, stimulating input 1 then input 2 and vice versa, and confirming that each input had EPSCs of identical amplitude irrespective of whether it came first or second. This technique is applicable for both depressing and facilitating synapses. The amplifier was a Multiclamp 700B. Dual, simultaneous recordings were used for recordings of non-converging inputs in Fig. 4. Synapses were allowed 10 s to recover from paired stimulation and 30 s from train stimulation. Drugs used were strychnine (10 μM, all AVCN recordings), bicuculline (25 μM, all cerebellar recordings), NBQX (10 μM, Fig. 4), MK-801 (4 μM, Fig. 4), and cyclothiazide (50 μM, Fig. 3).

To quantify plasticity for a synapse, we measured EPSCs under various conditions (pairs of pulses at different intervals, trains at different frequencies). Each stimulus condition was repeated ~5 times, and the EPSCs were averaged together. EPSCs were normalized to the initial, rested EPSC of each synapse. Each normalized EPSC was considered a measure (x_i), and the plasticity of a synapse was a collection of these measures, expressed as a vector: $\vec{x} = (x_1, x_2, \ldots, x_n)$. To quantify the difference in plasticity between two synapses ($\vec{x}$ and $\vec{y}$), we

calculated the Pythagorean distance between these vectors: $|\vec{x} - \vec{y}| = \sqrt{\sum_i (x_i - y_i)^2}$. To assess whether this similarity was significant for two converging synapses, we compared against distances between non-converging synapses, using the Kolmogorov-Smirnov test for statistical significance. This metric has a number of advantages. First, it is unbiased in terms of emphasizing different EPSC measures as carrying more information about plasticity than others. Second, the distance measure treats both endbulbs symmetrically. Asymmetrical comparisons, such as simple subtraction or ratios, would introduce bias. Third, any unanticipated bias in this calculation should also impact comparisons between non-converging endbulbs, so our statistical approach effectively removes this as a problem.

Results

We characterized plasticity by measuring normalized EPSC amplitudes for each synapse in response to pairs of pulses (Fig. 1Bi) as well as trains of 20 stimuli at physiologically-relevant AN firing rates (100, 200, and 333 Hz) (Sachs and Abbas, 1974). To compare plasticity of two endbulbs, we summed the squares of the difference between each EPSC amplitude, and took the square root (Fig. 1Bii). We refer to this as the “distance” between the endbulbs being compared. To decide if plasticity was similar, we compared the distance between endbulbs that converge onto the same BC against endbulbs that terminated on different BCs recorded from the same animal on the same day (Fig. 1A). This was an important refinement over our initial study (Yang and Xu-Friedman, 2009), as it avoided potential effects of variability between preparations.

We analyzed distances for these two populations using cumulative frequency histograms, and compared the distributions with the Kolmogorov-Smirnov test. Converging endbulbs were significantly more similar than non-converging endbulbs when the distance measure included paired-pulse ratio data (PPR, Fig. 1C), as well as low frequency trains (100 Hz, 20 pulses, Fig. 1D). When the distance measure only included data from higher frequency trains, converging synapses were not significantly more similar (Fig. 1E,F), perhaps because stochastic aspects of neurotransmitter release dominate EPSC measurements at higher frequency. When all EPSC measures were used, including PPR and trains of all frequencies, converging inputs were significantly more similar than non-converging endbulbs (Fig. 1G). This suggests that plasticity of multiple endbulbs forming synapses on the same BC is coordinated.

The measurements of similarity above considered EPSC amplitudes normalized to the initial, rested EPSC amplitude ($EPSC_1$), which emphasizes similarity in the probability of release (P_r). We also considered whether other aspects of neurotransmitter release were similar by considering $EPSC_1$ without normalization. There was no particular similarity in the absolute $EPSC_1$ amplitude of converging inputs (Fig. 2A). The relative amplitude of the smaller of two converging inputs varied from 20–100% of the larger (Fig. 2B). The distribution showed two modes, one near 100%, and one near 40%, with an overall average of 55 ± 5% (N_C = 27 pairs). Relative amplitudes of the two converging inputs seemed to be unrelated to absolute $EPSC_1$ amplitude, because this was found with both large and small EPSCs (flat lines in Fig. 2C). This suggests that the two modes visible in Fig. 2B do not reflect fundamentally different cell types. Furthermore, these results indicate that plasticity but not absolute EPSC amplitude is coordinated, suggesting this coordination relates to the computational characteristics of the synapse.

We wanted to know where the similarity in plasticity was expressed. Endbulb depression results from presynaptic as well as postsynaptic mechanisms (Oleskevich et al., 2000). Postsynaptic plasticity results from AMPAR desensitization (Isaacson and Walmsley, 1996),

and this seems like a simple mechanism of coordinating converging inputs by, for example, a given BC expressing AMPAR subtypes with similar desensitization kinetics at all synapses. However, desensitization only affects plasticity over short time intervals (~20 ms) (Yang and Xu-Friedman, 2008; Chanda and Xu-Friedman, 2010), so it could only account for a small part of coordinated plasticity. To test this possibility, we used cyclothiazide (CTZ), which specifically affects desensitization at the endbulb (Yang and Xu-Friedman, 2008; Chanda and Xu-Friedman, 2010). CTZ has the greatest effect on PPR over the first 20 ms after $EPSC_1$ (Fig. 3Ai), and also has its greatest effect early in trains. The remaining depression after applying CTZ (the CTZ-insensitive component) probably reflects a presynaptic form of depression. We hypothesized that if presynaptic characteristics were similar for converging endbulbs (e.g. P_r), that the CTZ-insensitive component of depression should be similar. In addition, if postsynaptic characteristics were similar for converging endbulbs, then the CTZ-sensitive component of depression should be similar. These two possibilities are not mutually exclusive.

We examined the CTZ-sensitive component by taking the difference before and after CTZ application for PPR or trains data (Fig. 3Aii). We found that the distances between converging endbulbs for this CTZ-sensitive component were significantly lower than for non-converging endbulbs (Fig. 3C). This indicated that the postsynaptic component of depression was similar for converging inputs. This finding could also be influenced by presynaptic characteristics, as the amount of desensitization depends on the amount of glutamate release as well as on postsynaptic characteristics such as receptor kinetics. We first tested this by analyzing the CTZ-insensitive component, by comparing PPR and trains in the presence of CTZ (Fig. 3Ai, closed symbols). In this experiment, converging inputs were not more similar than non-converging inputs (Fig. 3B). However, considering that the trend was in the direction of similarity, we tried a second approach to test for presynaptic similarity.

To better address whether the presynaptic aspects of synaptic transmission are similar between converging endbulbs, we compared P_r between endbulbs using the use-dependent blocker MK-801 (Hessler et al., 1993; Rosenmund et al., 1993). For non-converging inputs, two BCs were recorded at the same time, to ensure the drug conditions were identical (Fig. 4A). One AN input onto each BC was isolated, and then the plasticity of AMPA-receptor-mediated EPSCs was characterized. It was only practical to assess plasticity using PPR measurements, because of the limited duration of the experiment (Fig. 4A, top panel). Then the NMDA-receptor-mediated EPSC was measured at a holding potential of +40 mV in NBQX (Fig. 4A, bottom panel, insets). Once a stable baseline was recorded, MK-801 was applied, and each input was stimulated alternately every 10 s (Fig. 4A, bottom panels). MK-801 was applied until the NMDA EPSC became very reduced, and the decay of peak EPSC amplitude over trials was fit to an exponential function. A faster τ of decay indicates a higher P_r. For converging inputs, a single BC was recorded, and two AN inputs were isolated before measuring AMPA- and NMDA-receptor-mediated EPSCs similar to the previous experiment (Fig. 4B).

We compared simultaneously-recorded endbulbs, by considering the plasticity distance ($|PPR_1 - PPR_2|$) and the difference in τ_{decay}. Converging endbulbs had both similar PPR plasticity and similar τ_{decay} (open circles, Fig. 4C). By contrast, non-converging endbulbs had a wide range of PPR distances as well as a wide range of differences in τ_{decay} (closed squares, Fig. 4C). For non-converging endbulbs, the difference in τ_{decay} in MK-801 correlated strongly with the difference in AMPA PPR, further suggesting a specific relationship of each with P_r. The overall averages for converging and non-converging endbulbs were significantly different (crosses, Fig. 4C). These results indicated that converging endbulbs have similar presynaptic P_r.

An alternative explanation of these results could be that converging synapses have similar rate of decay in MK-801 because of glutamate spillover. One prediction of this would be, if glutamate spilled over between adjacent synapses, then the τ_{decay} for converging synapses should be faster than for non-converging synapses, which are quite distant and activated only every other stimulus trial. However, the rates of decay in MK-801 for converging (τ_{decay} = 10.8 ± 0.8 trials, N = 10) and non-converging endbulbs (τ_{decay} = 12.1 ± 1.3 trials, N = 14) are identical (P > 0.2, unpaired, one-tailed t-test). Thus, spillover does not appear to influence the assessment of P_r using MK-801. A second potential issue is NMDA receptor saturation, which does occur at the endbulb (Yang and Xu-Friedman, 2008). Saturation is only partial, as NMDA EPSCs during extended trains show significant temporal summation and are much larger than EPSCs following single stimuli (Pliss et al., 2009). Partial saturation could cause the relationship between P_r and τ_{decay} to differ from linearity, which would affect comparisons between both non-converging and converging synapses. However, converging endbulbs had similar τ_{decay} in MK-801, while non-converging endbulbs did not. Furthermore, these differences correlated with differences in plasticity. Therefore, partial NMDA receptor saturation does not prevent the relative assessment of P_r using MK-801.

To begin to understand how similarity is established, we examined when it emerges developmentally. We made similar measurements to those in Fig. 1 in mice before the onset of hearing (i.e. <P14). Stimulation of these young synapses at frequencies ≥200 Hz was somewhat less reliable, so we restricted the distance measure to PPR and 100 Hz train EPSCs (Fig. 5A). The distribution of distances between converging endbulbs overlapped with the distances between non-converging endbulbs, showing no significant difference (Fig. 5B). Before hearing onset, there was no difference between the overall mean converging and non-converging distances, but after the onset of hearing, the non-converging endbulbs were significantly more different than converging endbulbs, (Fig. 5C, D), as was seen with the larger metric in Fig. 1G. This could not result from the overall change in plasticity in Fig. 5B, because non-converging endbulbs are subject to the same maturation, yet have greater distances than converging endbulbs. We confirmed this using the MK-801 method of Fig. 4. Juvenile converging and non-converging endbulbs had similar differences in both PPR and τ_{decay} (Fig. 5E, P > 0.28, t-test, N_C = 5 pairs, N_{NC} = 5 pairs). There is an overall shift in plasticity over development (Fig. 5A), which may reflect an overall decrease in release probability. If this accounted for the coordination phenomenon, then the non-converging synapses should show also remain similar. In fact, they do not: converging synapses are more similar than non-converging synapses. Thus it cannot be a non-specific effect of changes in the population during ageing.

One possible explanation for these results is that these recordings are made from at least two separate populations of cells, that have distinct plasticity. In other words, it is possible that the coordinated plasticity we observe really reflects target-cell-specific synaptic plasticity. There are multiple types of BCs, that within cats have clearly defined differences in morphology and projection patterns (Osen, 1969; Cant and Morest, 1979). Recently two groups of BCs have been distinguished in mice, but their plasticity appears identical (Cao and Oertel, 2010). We verified whether we could detect multiple subtypes, by examining PPR for all endbulbs in the population studied. We saw no clusters of subgroups of endbulbs either in the entire PPR curve (Fig. 6A, top) nor for any interval plotted individually (Fig. 6A, bottom). Thus it appears that these recordings were from a uniform population of endbulbs.

We evaluated whether coordinated plasticity may represent a more general phenomenon by considering excitatory synapses in the cerebellum. Cerebellar synapses also undergo significant changes in young animals, maturing somewhat later than auditory synapses. We made recordings from Purkinje cells (PCs), stellate cells (SCs), and granule cells (GCs). We

could isolate and stimulate individual mossy fiber (MF) synapses onto GCs, but this was not practical for parallel fiber (PF) synapses onto PCs or SCs. Instead, we reasoned that if individual PFs were similar, then groups of PFs should also be similar, so we stimulated larger assemblies of PFs in the molecular layer, and assessed their similarity. We focussed on PPR data for the distance metric. Similar to the analysis of endbulbs in Fig. 6A, each synapse appeared to be drawn from a largely uniform populations of synapses (Fig. 6B-D).

We found that converging synapses in the cerebellum also showed similarity. The distances in plasticity between PF synapses onto the same PC were smaller than the distances for synapses onto different PCs (Fig. 7A). For PF synapses onto SCs in the molecular layer, this was not significant in slices from younger animals (P16–18, $P > 0.05$), but was significant in slices from older animals (P22, $P < 0.04$) (Fig. 7B). MF synapses onto GCs showed a similar developmental effect: converging inputs were not particularly similar in slices from younger animals (P14–17, $P > 0.2$), but were in older animals (P23–26, $P < 0.02$) (Fig. 7C). The age at which this shift took place was older in the cerebellum than the cochlear nucleus (i.e. ~P14, Fig. 5). These results suggest that coordinated plasticity could be a common feature among converging synapses in the nervous system. Furthermore, it suggests that the coordination mechanism does not require axosomatic synapses such as endbulbs, or synapses in direct proximity, but can also occur when synapses are located on disparate parts of the dendritic arbor.

Discussion

We show here a previously unknown form of synaptic regulation, in which synaptic inputs that converged on the same postsynaptic cell had similar short-term plasticity. For AN fibers, this appeared to arise through a similarity in presynaptic release probability (P_r). Furthermore, the similarity emerged after the onset of hearing for AN fibers, and even later for cerebellar PF and MF synapses. The coordinated plasticity we observed differs from target-cell-specific synaptic plasticity (Markram et al., 1998; Reyes et al., 1998; Rozov et al., 2001), which has been described comparing synapses onto different target cell types. We observed regulation on the scale of individual cells. This could confer distinct computational properties to individual neurons, effectively yielding a diverse population at the functional level.

Our findings raise questions about how plasticity becomes coordinated. The converging synapses have the postsynaptic cell in common, yet, at least for endbulbs, it is the presynaptic P_r that is similar (Fig. 4). This could involve some retrograde signal from the common postsynaptic cell instructing the presynaptic side to adjust P_r. Alternatively, it could be that the presynaptic fibers share some other characteristic that correlates with P_r. One possibility is the tonotopic origin in the cochlea, but this is unlikely because plasticity shows no organization along the tonotopic axis in the AVCN. Another possibility is that AN fibers with similar spontaneous firing rate converge on the same cell (Ryugo and Sento, 1991). This could account for the coordination we observe, provided P_r is regulated by activity, such as has been suggested in hippocampal cell culture (Branco et al., 2008). Indeed, endbulbs in deaf strains of mice appear to have different P_r from hearing strains (Oleskevich and Walmsley, 2002), so this is a plausible mechanism.

A second issue is whether the plasticity of converging inputs converges over development, or whether the plasticity of non-converging synapses diverges. The distances between non-converging synapses appear smaller before the onset of hearing than after the onset of hearing (compare the grey lines in Figs. 5C and D). This is particularly striking for the MK-801 experiments, in which older synapses show a wide range of differences in plasticity and τ_{decay} (compare Figs. 4D and 5E). In other words, it may be that converging endbulbs

retain similarity over development, while non-converging endbulbs become more diverse. This poses the same essential problem of how endbulbs are stabilized, but it may reflect quite different computational goals.

It is a question how coordinated plasticity would interact with the various forms of long-term plasticity, which are thought to underlie learning and memory. When the expression of long-term plasticity is postsynaptic (through changes in receptor number), induction would not be expected to change short-term plasticity (e.g. Manabe and Nicoll, 1994). However, synapses that express presynaptic forms of long-term plasticity would undergo changes in P_r and short-term plasticity. Long-term plasticity has not been described at the endbulb, but PF synapses show both pre- and post-synaptic mechanisms of expression (Jorntell and Hansel, 2006), and MF synapses show presynaptic mechanisms of expression (Sola et al., 2004). It is not yet clear whether these mechanisms support/cause coordinated plasticity or interfere with it.

One issue for evaluating whether this phenomenon is present at additional synapses is the sensitivity of our approach. This was impacted by the fact that measures of short-term plasticity are inherently variable, which likely added noise to our distance measurement. Furthermore, this is essentially a phenomenon of residual variance. Plasticity is primarily set by the cell types forming the synapse (i.e. target-cell-specific synaptic plasticity). What we quantified here was what remained after that, that is, the synapses that form on the same cell deviated from the mean in the same way. Comparing variances requires larger sample sizes than comparing means. These detection issues compounded the technical challenges of isolating distinct axons or pathways in brain slices, and may make studying other synapses challenging.

Coordinated plasticity is likely to have functional consequences. Starting EPSC amplitudes are not particularly similar in converging inputs (Fig. 2), so it appears that what is being coordinated is not the strength of the synapse per se, but rather how the strength of the synapse changes with activity. This would produce synapses that filter presynaptic activity in common ways. We have investigated the effects of different degrees of depression using dynamic clamp (Yang and Xu-Friedman, 2009). The present results suggest coordinated plasticity would yield a diverse population of BCs sensitive to different temporal aspects of presynaptic activity.

Questions have been raised recently about the importance of plasticity to neuronal function, at least in part because spontaneous activity may reduce the importance of the rested, initial P_r (Hermann et al., 2007; Lorteije et al., 2009; Wang et al., 2010). If plasticity were unimportant, one might expect it to be random, but our results indicate that this is not the case, and it is in fact tightly regulated. Thus, coordinated plasticity provides indirect evidence that the initial P_r plays an important functional role in the auditory pathway and the cerebellum.

We found that plasticity becomes coordinated after the onset of hearing for the endbulb, and somewhat later in the cerebellum, perhaps as locomotor behavior develops. We do not yet know if this requires activity (spontaneous or sound-driven), or simply ageing. Synaptic maturation in the visual system seems highly dependent on visual experience around the time of eye-opening (Lu and Constantine-Paton, 2004). Homeostatic processes influence mEPSC amplitudes (Turrigiano et al., 1998), and have also been suggested to play a role in setting P_r on different branches of cultured hippocampal neurons (Branco et al., 2008). We find yet greater uniformity in our acute brain slices, in which axosomatic synapses (AN→BC) and synapses onto separate dendrites (MF→GC) are coordinated.

Acknowledgments

The authors thank S. Chanda, A. Fischer, T. Jarsky, T. Ngodup, D. Power, T. Ruan, and Y. Yang for helpful comments and discussion during the project. This work was supported by NIH grant R01 DC008125 to MAXF.

References

Abbott LF, Regehr WG. Synaptic computation. Nature. 2004; 431:796–803. [PubMed: 15483601]

Abbott LF, Varela JA, Sen K, Nelson SB. Synaptic depression and cortical gain control. Science. 1997; 275:220–224. [PubMed: 8985017]

Branco T, Staras K, Darcy KJ, Goda Y. Local dendritic activity sets release probability at hippocampal synapses. Neuron. 2008; 59:475–485. [PubMed: 18701072]

Cant NB, Morest DK. Organization of the neurons in the anterior division of the anteroventral cochlear nucleus of the cat. Light-microscopic observations. Neuroscience. 1979; 4:1909–1923. [PubMed: 530438]

Cao XJ, Oertel D. Auditory nerve fibers excite targets through synapses that vary in convergence, strength, and short-term plasticity. J Neurophysiol. 2010; 104:2308–2320. [PubMed: 20739600]

Chanda S, Xu-Friedman MA. A low-affinity antagonist reveals saturation and desensitization in mature synapses in the auditory brainstem. J Neurophysiol. 2010; 103:1915–1926. [PubMed: 20107122]

Chen C, Regehr WG. Developmental remodeling of the retinogeniculate synapse. Neuron. 2000; 28:955–966. [PubMed: 11163279]

Fortune ES, Rose GJ. Roles for short-term synaptic plasticity in behavior. J Physiol Paris. 2002; 96:539–545. [PubMed: 14692501]

Hermann J, Pecka M, von Gersdorff H, Grothe B, Klug A. Synaptic transmission at the calyx of Held under in vivo like activity levels. J Neurophysiol. 2007; 98:807–820. [PubMed: 17507501]

Hessler NA, Shirke AM, Malinow R. The probability of transmitter release at a mammalian central synapse. Nature. 1993; 366:569–572. [PubMed: 7902955]

Isaacson JS, Walmsley B. Amplitude and time course of spontaneous and evoked excitatory postsynaptic currents in bushy cells of the anteroventral cochlear nucleus. J Neurophysiol. 1996; 76:1566–1571. [PubMed: 8890276]

Jorntell H, Hansel C. Synaptic memories upside down: bidirectional plasticity at cerebellar parallel fiber-Purkinje cell synapses. Neuron. 2006; 52:227–238. [PubMed: 17046686]

Joshi I, Wang LY. Developmental profiles of glutamate receptors and synaptic transmission at a single synapse in the mouse auditory brainstem. J Physiol. 2002; 540:861–873. [PubMed: 11986375]

Limb C, Ryugo DK. Development of primary axosomatic endings in the anteroventral cochlear nucleus of mice. J Assoc Res Otolaryngol. 2000; 1:103–119. [PubMed: 11545139]

Lorente de Nó, R. The Primary Acoustic Nuclei. New York: Raven Press; 1981.

Lorteije JA, Rusu SI, Kushmerick C, Borst JG. Reliability and precision of the mouse calyx of Held synapse. J Neurosci. 2009; 29:13770–13784. [PubMed: 19889989]

Lu W, Constantine-Paton M. Eye opening rapidly induces synaptic potentiation and refinement. Neuron. 2004; 43:237–249. [PubMed: 15260959]

Manabe T, Nicoll RA. Long-term potentiation: evidence against an increase in transmitter release probability in the CA1 region of the hippocampus. Science. 1994; 265:1888–1892. [PubMed: 7916483]

Markram H, Wang Y, Tsodyks M. Differential signaling via the same axon of neocortical pyramidal neurons. Proc Natl Acad Sci USA. 1998; 95:5323–5328. [PubMed: 9560274]

Oleskevich S, Walmsley B. Synaptic transmission in the auditory brainstem of normal and congenitally deaf mice. J Physiol. 2002; 540:447–455. [PubMed: 11956335]

Oleskevich S, Clements J, Walmsley B. Release probability modulates short-term plasticity at a rat giant terminal. J Physiol. 2000; 524:513–523. [PubMed: 10766930]

Osen KK. Cytoarchitecture of the cochlear nuclei in the cat. J Comp Neurol. 1969; 136:453–484. [PubMed: 5801446]

Pliss L, Yang H, Xu-Friedman MA. Context-dependent effects of NMDA receptors on precise timing information at the endbulb of held in the cochlear nucleus. J Neurophysiol. 2009; 102:2627–2637. [PubMed: 19726731]

Reyes A, Lujan R, Rozov A, Burnashev N, Somogyi P, Sakmann B. Target-cell-specific facilitation and depression in neocortical circuits. Nat Neurosci. 1998; 1:279–285. [PubMed: 10195160]

Rosenmund C, Clements JD, Westbrook GL. Nonuniform probability of glutamate release at a hippocampal synapse. Science. 1993; 262:754–757. [PubMed: 7901909]

Rozov A, Burnashev N, Sakmann B, Neher E. Transmitter release modulation by intracellular Ca^{2+} buffers in facilitating and depressing nerve terminals of pyramidal cells in layer 2/3 of the rat neocortex indicates a target cell-specific difference in presynaptic calcium dynamics. J Physiol (Lond). 2001; 531:807–826. [PubMed: 11251060]

Ryugo DK, Fekete DM. Morphology of primary axosomatic endings in the anteroventral cochlear nucleus of the cat: a study of the endbulbs of Held. J Comp Neurol. 1982; 210:239–257. [PubMed: 7142440]

Ryugo DK, Sento S. Synaptic connections of the auditory nerve in cats: relationship between endbulbs of Held and spherical bushy cells. J Comp Neurol. 1991; 305:35–48. [PubMed: 2033123]

Sachs MB, Abbas PJ. Rate versus level functions for auditory-nerve fibers in cats: tone-burst stimuli. J Acoust Soc Am. 1974; 56:1835–1847. [PubMed: 4443483]

Sola E, Prestori F, Rossi P, Taglietti V, D'Angelo E. Increased neurotransmitter release during long-term potentiation at mossy fibre-granule cell synapses in rat cerebellum. J Physiol. 2004; 557:843–861. [PubMed: 15090602]

Taschenberger H, von Gersdorff H. Fine-tuning an auditory synapse for speed and fidelity: developmental changes in presynaptic waveform, EPSC kinetics, and synaptic plasticity. J Neurosci. 2000; 20:9162–9173. [PubMed: 11124994]

Taschenberger H, Leão RM, Rowland KC, Spirou GA, von Gersdorff H. Optimizing synaptic architecture and efficiency for high-frequency transmission. Neuron. 2002; 36:1127–1143. [PubMed: 12495627]

Turrigiano GG, Leslie KR, Desai NS, Rutherford LC, Nelson SB. Activity-dependent scaling of quantal amplitude in neocortical neurons. Nature. 1998; 391:892–896. [PubMed: 9495341]

Wall MJ. Short-term synaptic plasticity during development of rat mossy fibre to granule cell synapses. Eur J Neurosci. 2005; 21:2149–2158. [PubMed: 15869511]

Wang Y, Ren C, Manis PB. Endbulb synaptic depression within the range of presynaptic spontaneous firing and its impact on the firing reliability of cochlear nucleus bushy neurons. Hear Res. 2010; 270:101–109. [PubMed: 20850512]

Xu-Friedman MA, Regehr WG. Dynamic-clamp analysis of the effects of convergence on spike timing. I. Many synaptic inputs. J Neurophysiol. 2005; 94:2512–2525. [PubMed: 16160092]

Yang H, Xu-Friedman MA. Relative roles of different mechanisms of depression at the mouse endbulb of Held. J Neurophysiol. 2008; 99:2510–2521. [PubMed: 18367696]

Yang H, Xu-Friedman MA. Impact of synaptic depression on spike timing at the endbulb of Held. J Neurophysiol. 2009; 102:1699–1710. [PubMed: 19587324]

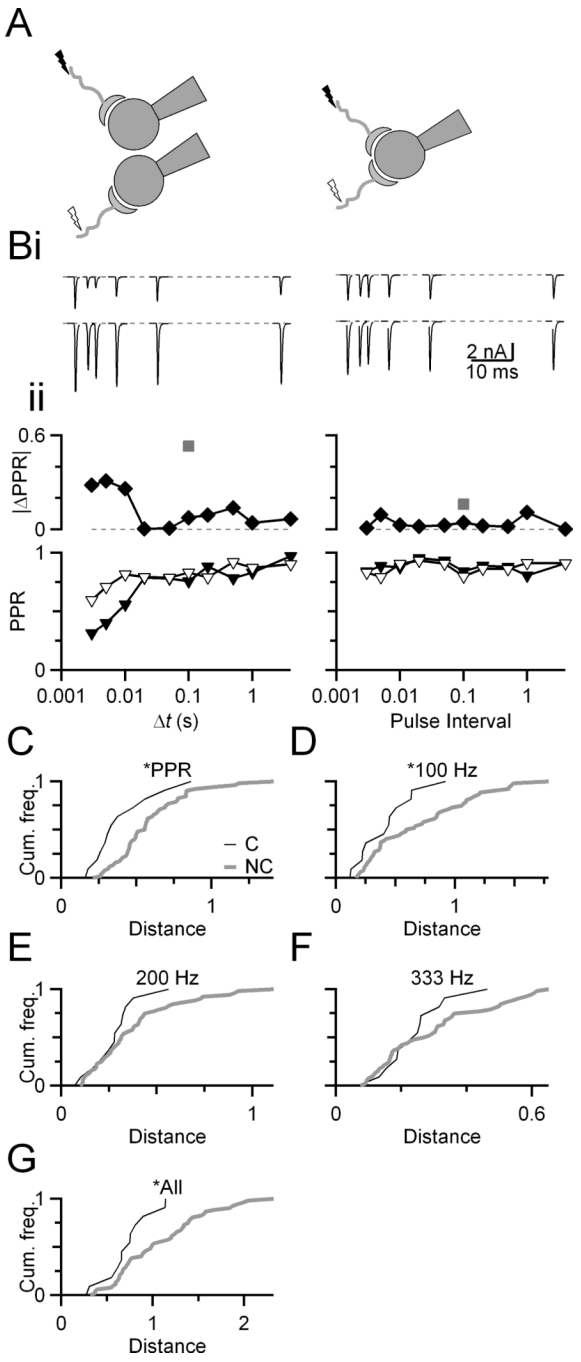

Figure 1.

Converging inputs are similar. **A**, Diagram of experimental arrangement. Recordings were made from auditory nerve (AN) fiber synapses that converge on the same bushy cell (BC) or onto different BCs. **B**, Representative voltage-clamp experiments of converging and non-converging endbulb EPSCs. **i**, EPSCs resulting from stimulating individual inputs (top vs. bottom traces) at different paired-pulse intervals. **ii**, Quantification of short-term plasticity using the paired-pulse ratio (PPR = $EPSC_2/EPSC_1$). PPR for individual endbulbs is shown by triangles in the lower panel. The absolute difference between these two curves is plotted in the upper panel (diamonds). The square root of the sum of squares of these values is

termed the “distance” between the endbulbs (grey squares). **C–G**, Cumulative frequency histograms of distances between converging (black) and non-converging (grey) endbulbs (**C**) PPR, or using a similar analysis for trains of 20 stimuli at (**D**) 100, (**E**) 200, or (**F**) 333 Hz. An overall distance incorporating all PPR and trains measures is shown in **G**. The distributions in **C**, **D**, and **G** are significantly different (Kolmogorov-Smirnov test (KS-test), $P < 0.05$, number of converging endbulbs $N_C = 12$ pairs, number of non-converging endbulbs $N_{NC} = 53$ pairings). Slices are from mice aged P18–21.

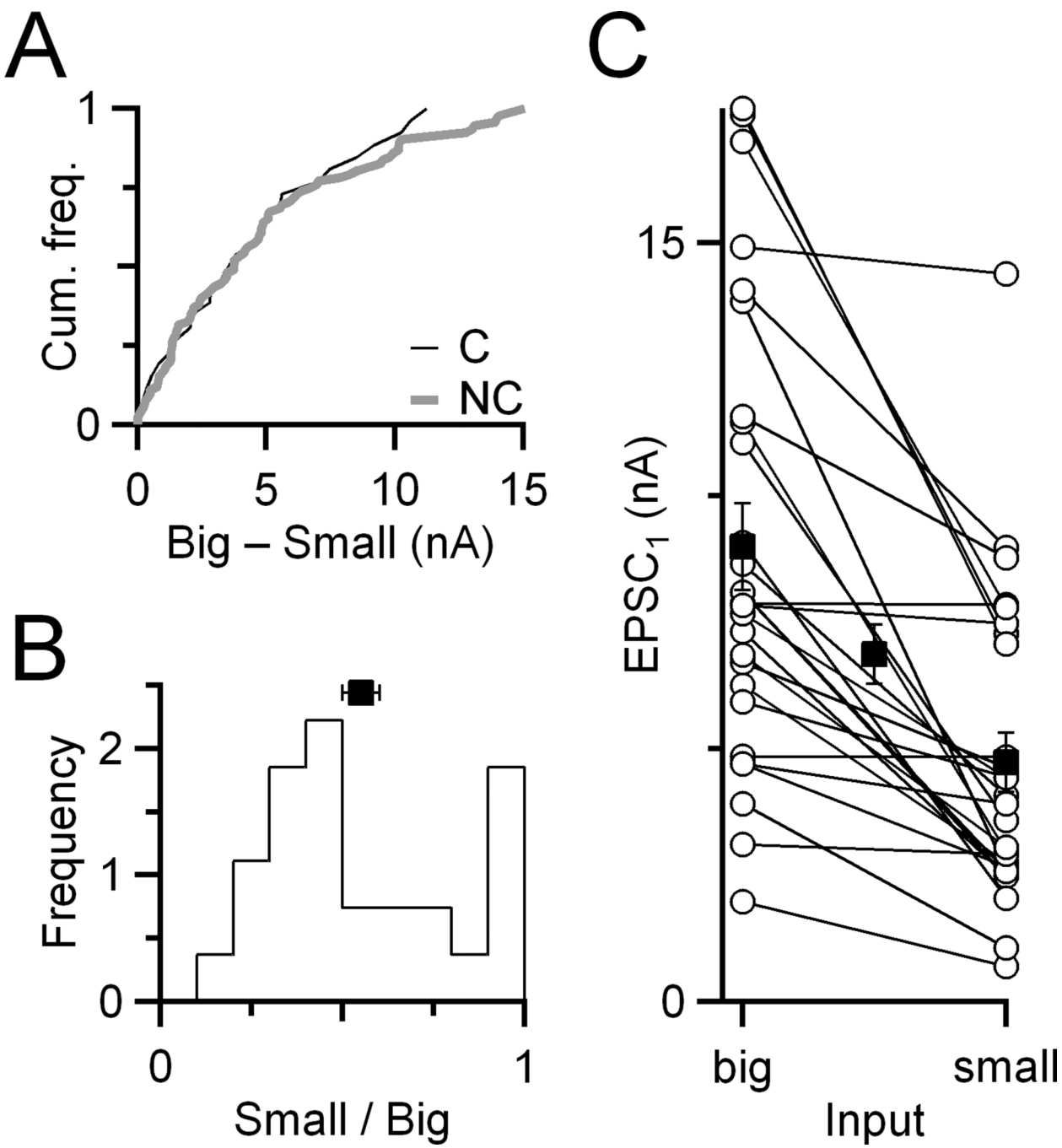

Figure 2.

Coordinated plasticity is not reflected in similarity in initial EPSC ($EPSC_1$). **A**, Cumulative frequency histogram of difference in $EPSC_1$ for converging *vs.* non-converging inputs. There is no significant difference ($P > 0.95$, K-S test, $N_C = 27$ pairs, $N_{NC} = 93$ pairings). **B**, Relative amplitudes of converging endbulbs ($N_C = 27$ pairs). The relatively smaller input is scaled to the larger one. The population average is indicated by the square (mean ± standard error of the mean (SEM)). **C**, Relationships between the absolute $EPSC_1$ amplitudes for converging endbulbs. Open circles indicate amplitudes of individual endbulbs. Converging

endbulbs are connected by lines. Closed squares indicate average amplitudes of relatively larger and smaller endbulbs in the pair, as well as the overall average (middle square).

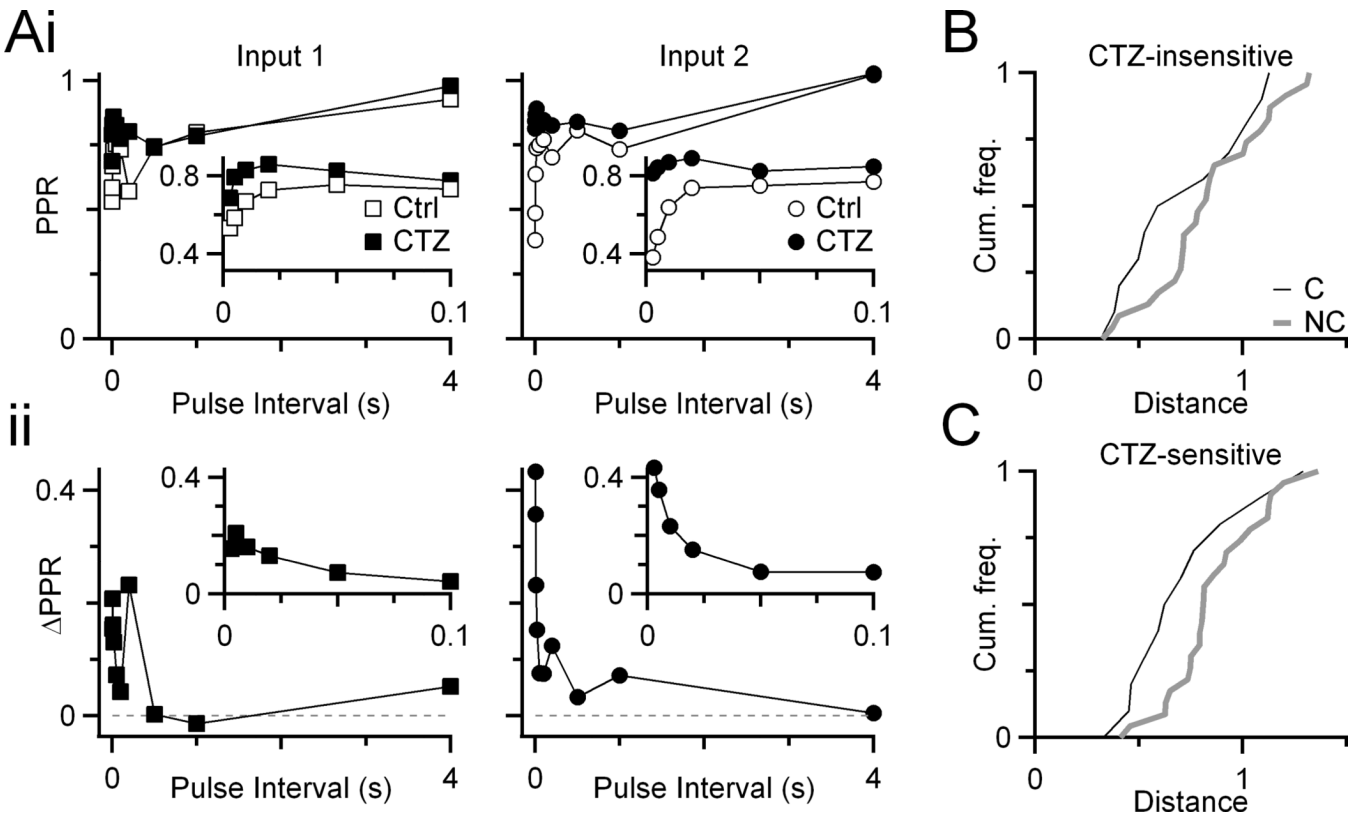

Figure 3.

Effects of cyclothiazide (CTZ) on similarity of converging endbulbs. **Ai**, Representative experiment of two converging inputs (left and right panels), before and after treatment with 50 μM CTZ. **ii**, The change in PPR (ΔPPR) resulting from CTZ for the two endbulbs. Insets show PPR and ΔPPR at short intervals. **B**, Cumulative histogram of plasticity distances for converging and non-converging endbulbs in the presence of CTZ (i.e. solid symbols of panel **Ai**). The distance measure incorporates PPR as well as EPSC amplitudes from the initial 7 pulses during 100, 200, and 333 Hz trains when desensitization is significant (Chanda and Xu-Friedman, 2010) (i.e. $\text{Distance}=\sqrt{\sum(\text{EPSC}_{\text{AN1}}^{\text{CTZ}}-\text{EPSC}_{\text{AN2}}^{\text{CTZ}})^2}$). The difference in distributions is not significant (K-S test: $P = 0.16$, $N_C = 11$, $N_{NC} = 24$). **C**, Cumulative frequency plot of the CTZ-sensitive component of plasticity. Responses in CTZ were subtracted from control (as in panel **Aii**), and distances were computed between those differences (i.e. $\text{Distance}=\sqrt{\sum(\Delta\text{EPSC}_{\text{AN1}}-\Delta\text{EPSC}_{\text{AN2}})^2}$). Converging endbulbs have significantly lower distances than non-converging endbulbs (K-S test: $P < 0.05$, $N_C = 11$ pairs, $N_{NC} = 24$ pairings). Slices are from mice aged P16–21.

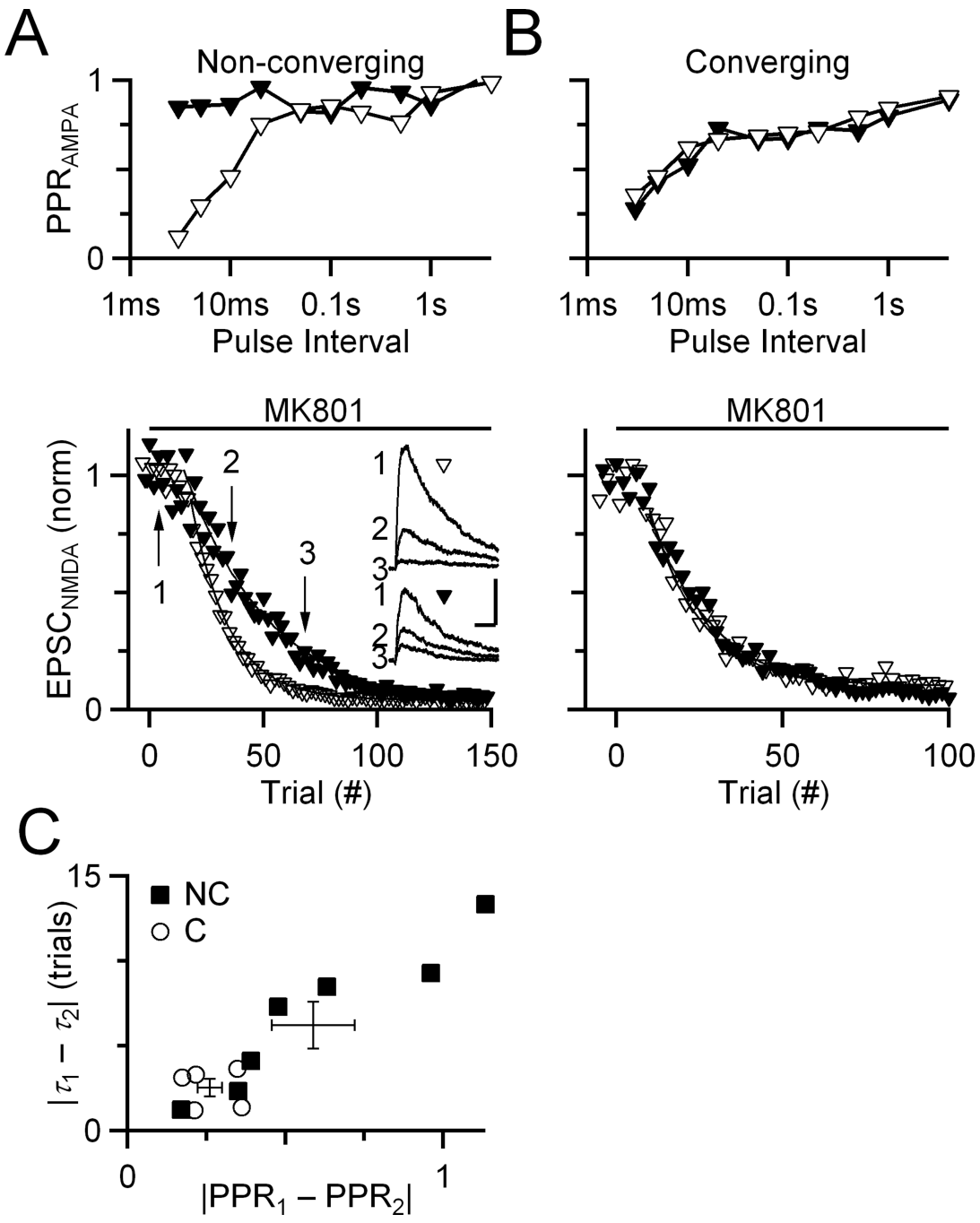

Figure 4.

Experiments using MK-801 indicate that converging endbulbs have similar probability of presynaptic neurotransmitter release. **A, B**, Representative experiments showing the effects of MK-801 on converging and non-converging endbulbs. Top panels, PPR curves for two endbulbs that end on (a) two simultaneously recorded BCs (**B**) or a single BC, held at −70 mV. Bottom panels, Effects of MK-801 on NMDA-receptor-mediated EPSCs for non-converging (**A**) or converging (**B**) endbulbs. To measure NMDA EPSCs, BCs were held at +40 mV in the presence of NBQX. Inputs were stimulated alternately every 10 s. Arrows indicate the timing of the NMDA EPSCs shown in the inset. Lines are exponential fits to the

data used for measuring the **τ** of decay. Inset scale bars are 10 ms and 0.5 nA. **C**, Correlation between similarity in PPR and in decay of NMDA EPSC. The abscissa is the distance between PPR curves (as in Fig. 1**C**). The ordinate is the difference in the τ_{decay} from experiments similar to panels (**A**) and (**B**). Converging endbulbs cluster at low distance values, while non-converging endbulbs are more widely distributed in both measures. Crosses show the population averages, which are significantly different ($P < 0.05$, *t*-test, $N_C = 5$ pairs, $N_{NC} = 7$ pairs). Slices are from mice aged P16–21.

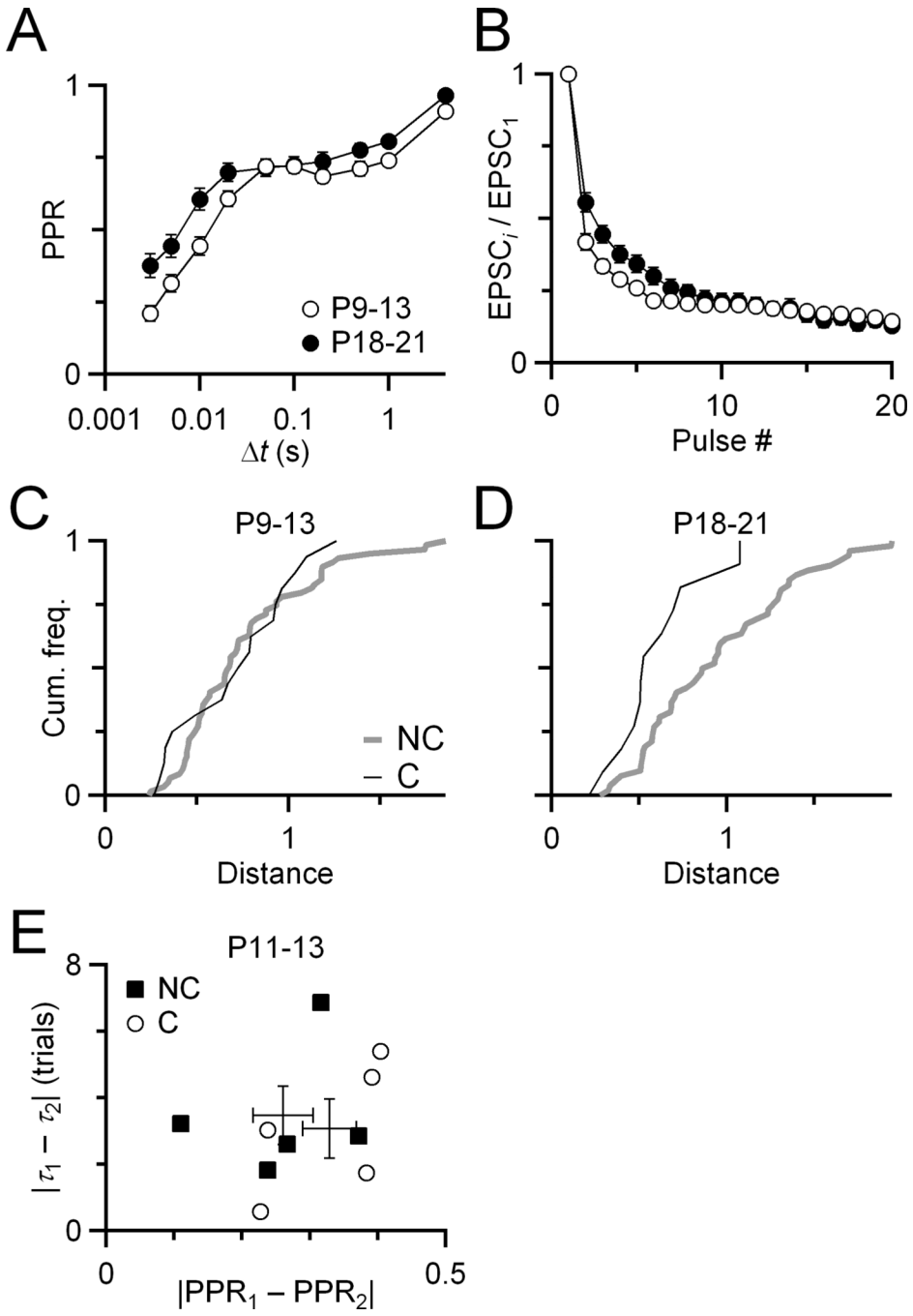

Figure 5.

Coordinated plasticity emerges after the onset of hearing. **A,B**, Plasticity changes over development, with a small decrease in depression seen both for pairs of pulses (**A**) and during 100 Hz trains (**B**). Data for P9–13 are from 17 endbulbs, and for P18–21 are from 12 endbulbs. **C**, Cumulative frequency plot of distance for converging and non-converging endbulbs before the onset of hearing. The two curves are not significantly different (K-S test, $P > 0.5$, $N_C = 17$ pairs, $N_{NC} = 60$ pairings). The distance metric includes PPR and 100 Hz trains measurements. For comparison, the same distance metric for endbulbs after the onset of hearing (**D**), which is significantly different ($P < 0.04$, $N_C = 12$ pairs, $N_{NC} = 53$

pairings). **E**, MK-801 experiment similar to Fig. 4, but in juvenile endbulbs. The converging and non-converging populations overlap considerably, indicating no particular similarity of endbulbs before the onset of hearing ($P > 0.28$, *t*-test, $N_C = 5$ pairs, $N_{NC} = 5$ pairs).

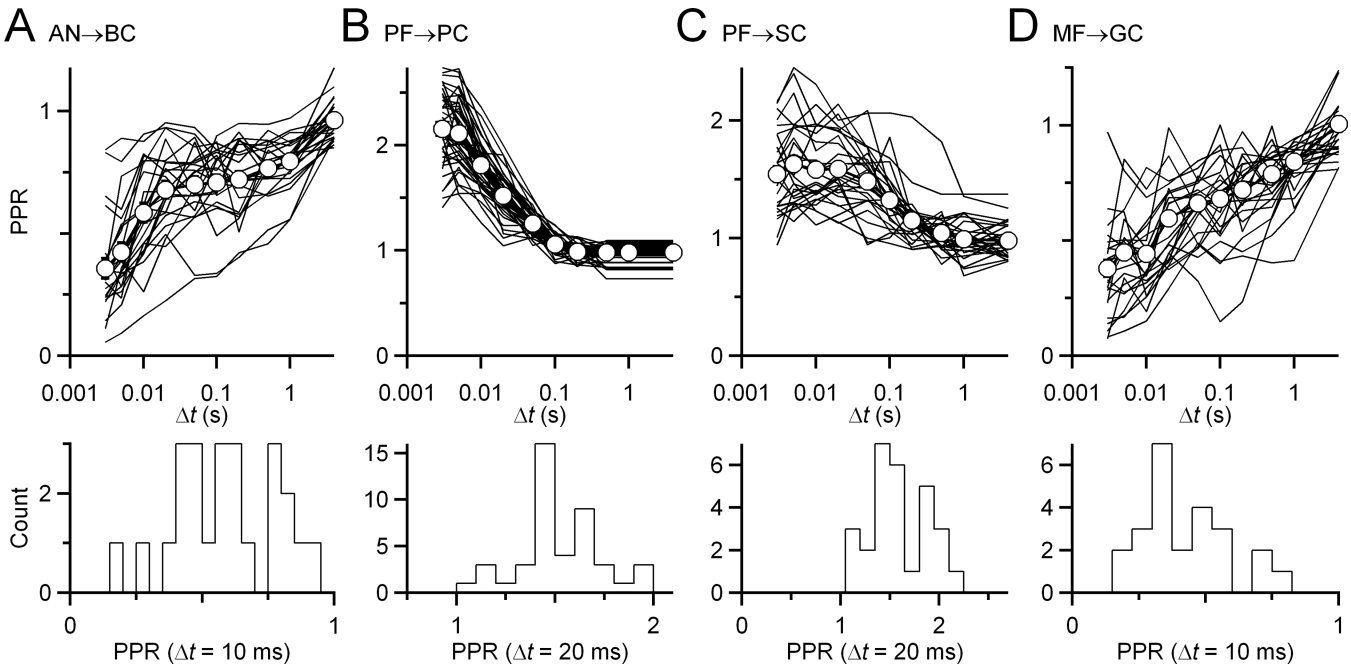

Figure 6.

Plasticity in each population of recorded cells is unimodally distributed. Top panels, Paired pulse recovery curves for all characterized synapses (AN→BC (**A**), mossy fiber to granule cell MF→GC (**D**)) or pathways (parallel fiber to Purkinje cell PF→PC (**B**), parallel fiber to stellate cell PF→SC (**C**)). Each line represents a separate synapse or pathway. Open circles and bold lines are population averages. There is considerable variability in plasticity across each population. Bottom panels, Representative histograms at individual time intervals when plasticity is particularly strong. No measure shows multiple modes, suggesting that each group of recordings is drawn from an effectively uniform population.

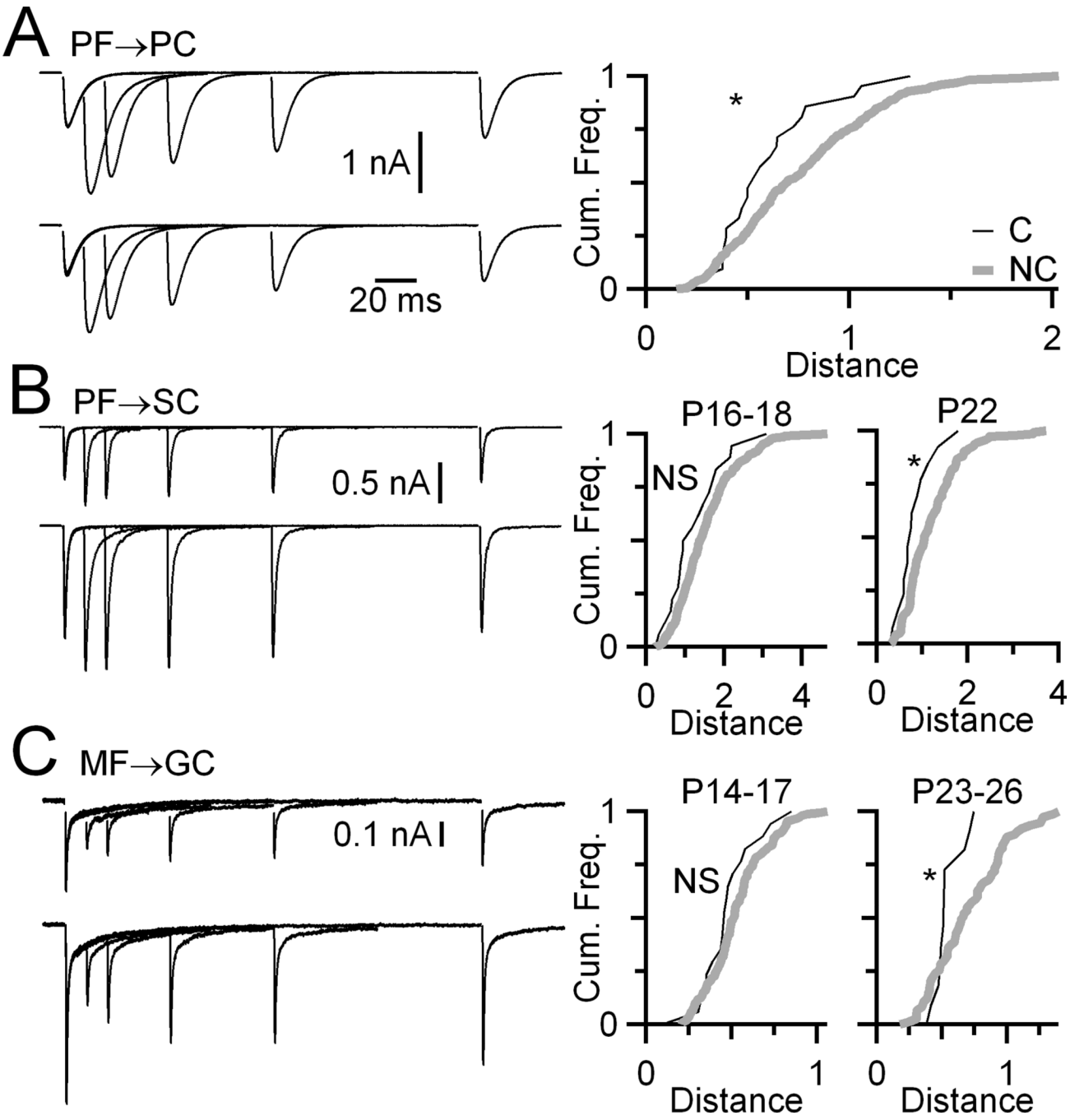

Figure 7.

Synapses in the cerebellum show similarity in converging inputs. Representative traces from individual pathways or synapses are shown on the left. Comparisons between converging and non-converging synapses are shown on the right. The synapses considered were (**A**) PF→PC, (**B**) PF→SC, and (**C**) MF→GC. Coordinated plasticity for MF→GC and PF→SC terminals was only significant in older synapses. The K-S statistical results are (**A**) PF→PC: P16–19, $P < 0.04$, $N_C = 22$ pairs, $N_{NC} = 348$ pairings, (**B**) PF→SC: P16–18, $P > 0.05$, $N_C = 19$ pairs, $N_{NC} = 348$ pairings, and P22 (3 preparations), $P < 0.03$, $N_C = 14$ pairs, $N_{NC} = 144$

pairings, (**C**) MF→GC: P14–17, $P > 0.2$, N_C =18 pairs, N_{NC} = 152 pairings, and P23–26, $P < 0.02$, N_C = 12 pairs, N_C = 76 pairings.